Root and contact stress calculations in surface densified PM gears

Anders Flodin[1], Linnea Fordén
Höganäs AB, 26383 Höganäs, Sweden

Abstract

Powder metallurgy a.k.a PM in combination with surface densification by radial cold rolling is a competitive manufacturing method for high performance gears compared to producing gears by turning, hobbing and shaving. This paper aims to give a deeper understanding regarding density and stress distribution in a surface densified and case hardened PM gear tooth. The results from the calculations are presented and the design aspect of surface densified components will be discussed.

Introduction

A successful and well-known method to improve static and dynamic properties of a part made from both PM and wrought steel is to introduce compressive stresses in the surface of the part. For PM material, it is also of interest to increase density since Young's modulus E, poisson's ratio ν, and fatigue properties will be improved. This paper therefore focuses on the method of surface densification applied to gearwheels made from PM material and how the stress distribution in a loaded gear tooth is affected by the surface densification and case hardening. This will be investigated by calculations of root stress and contact stress using Finite Element Analysis, FEA.

Modelling the densified layer

In a surface densified PM material the density in a thin layer around the tooth flank and root will be increased to fully dense on the surface and then gradually decreasing to the core density over a distance of around 1 mm. Data used in figure 1b from in-house measurement.

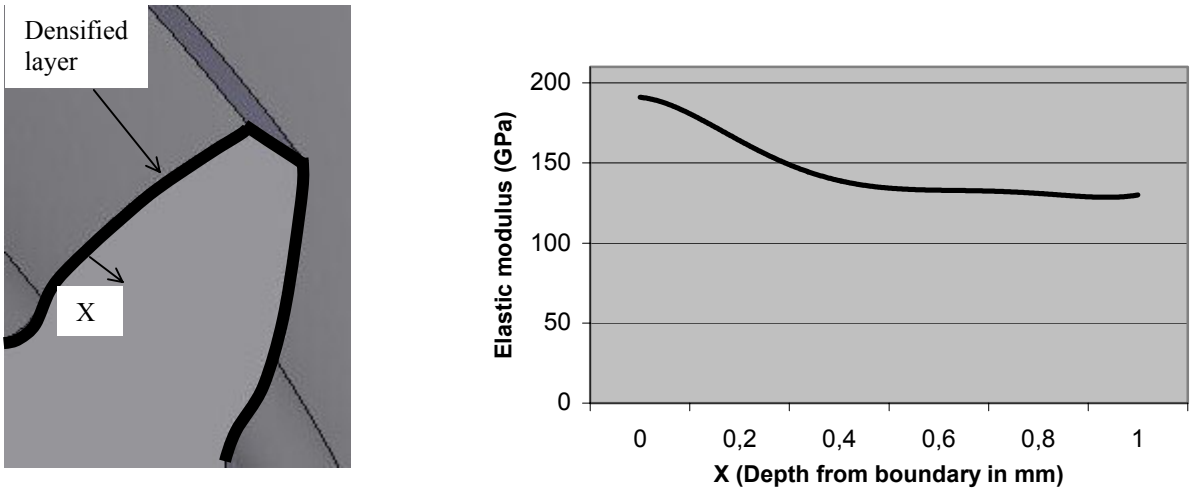


Figure 1. a) Illustration of densified layer. b) Variation of Elastic modulus with x.

The typical variation of E and υ is described by equation 1 and 2 respectively where ρ is sintered density, ρ_0 and ν_0 is wrought steel density and poission's ratio respectively, see [1,2].

[1] Corresponding author: anders.flodin@hoganas.com

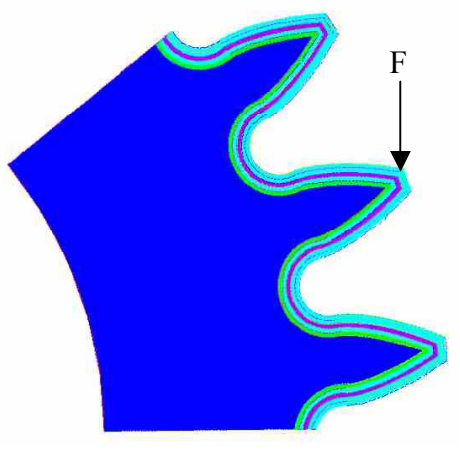
$$E = E_0 \cdot \left(\frac{\rho}{\rho_0} \right)^{3.4} \quad (1)$$

$$\upsilon = \left(\frac{\rho}{\rho_0} \right)^{0.16} (1 + \upsilon_0) - 1 \quad (2)$$

The effect the increased Young's modulus has on the stress distribution can be modelled by different FE approaches. In this paper, thin layers have been used; each with a different E and ν according to equation 1 and 2. In total there are 5 layers with a width of 0.2 mm plus the bulk material, i.e. 6 materials, see figure 2b. The layers are bonded to each other, no sliding or separation occurs between the different layers.

Layer number and density	E-mod. GPa	Poison's ratio
1 (7.64g/cm^3)	192	0.282
2 (7.5g/cm^3)	180	0.278
3 (7.35g/cm^3)	168	0.274
4 (7.03g/cm^3)	145	0.265
5 (6.96g/cm^3)	140	0.263
Core (pure PM) (6.95g/cm^3)	139	0.262

a)



b)

Figure 2. a) Material data, from eq. 1 and 2. b) Section of gear with 5 layers.

Modelling the gear

Although the contact problem at hand is fully three dimensional, a two dimensional FE mesh is used since it reduces the solution time and simplifies evaluation. Since, at mid tooth width, a 2D residual stress field can be assumed in the normal plane shown by figure 2b, the FE-mesh should be created to model the normal cross section of the helical gear. This is quite complicated since the tooth form in the normal plane is not described by an involute. This paper is not focusing on a specific gear but gears in general. Therefore the tooth form in the normal plane is described by a spline curve modelling an involute. This assumption will have little or no effect as long as the helix angle is low or moderate. The 2D approach assumes plain strain, which is valid, according to Pehan et al. [3], as long as the tooth width is greater than 6 times the module of a standard gear geometry. It is also common practice to include 3 teeth in the model in order to capture the boundary conditions right, see [3,4,5].

Modelling contact

Resolving the stress distribution on the surface assuming Hertzian contact conditions and an isotropic material is well described in literature. The stress distribution below the contact zone is analytically solvable using equations derived by Mc Ewen [6] and others. When the contact becomes non Hertzian, numerical methods have to be applied, see [7]. Surface densification creates anisotropic material behaviour. Here the anisotropy is captured by the different isotropic layers. The different E and ν will imply boundary effects between the layers with stepwise changes in plane layer stresses. A more refined layer approach will minimise the boundary effects; this paper demonstrates the method applied to an ideal gear contact. In this

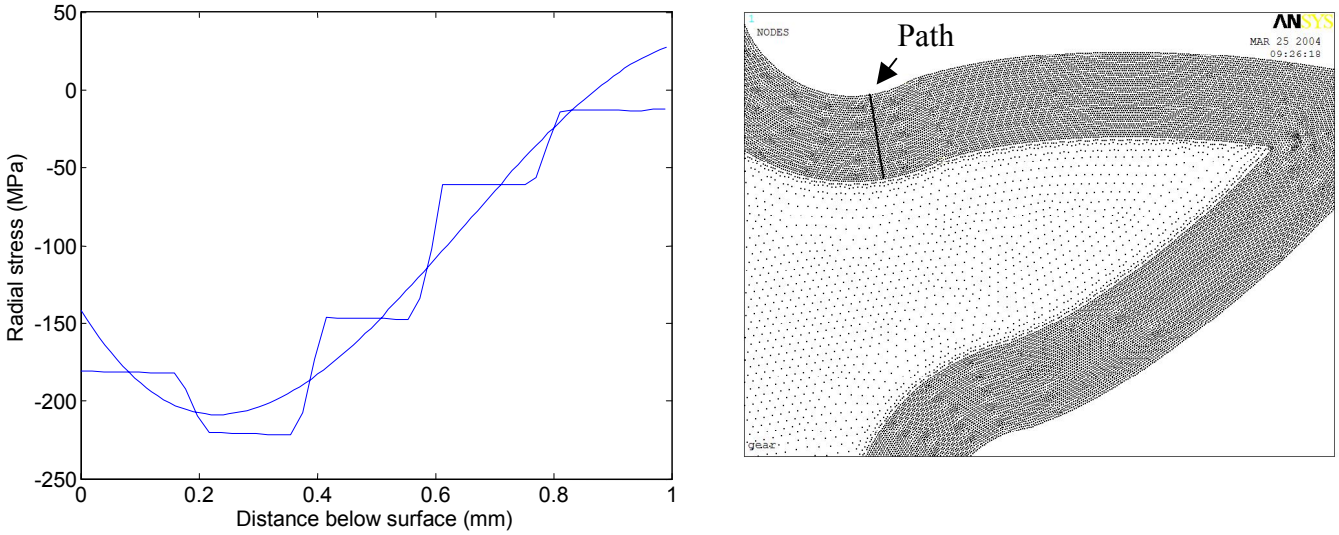
paper a constant load corresponding to a maximum Hertzian stress level in a wrought material of approximately 1.5 GPa is used in the contact calculations.

Modelling residual stresses

The residual stresses from case hardening have been modelled using a similar technique to [3]. Different thermal expansion coefficients are applied to the different layers and a varying temperature load is applied. With a higher expansion coefficient in the outer layers, compressive stresses are obtained at the surface and tension occurs in the core. The stresses have been measured using X-ray diffraction on a similar gear to the one being modelled, and the model has been tuned to match the measured stress levels.

Results

As mentioned previously, the root stress from bending and subsurface stress from the contact are the most important design parameters. The root stress is composed by stress from bending and residual stress from case hardening.

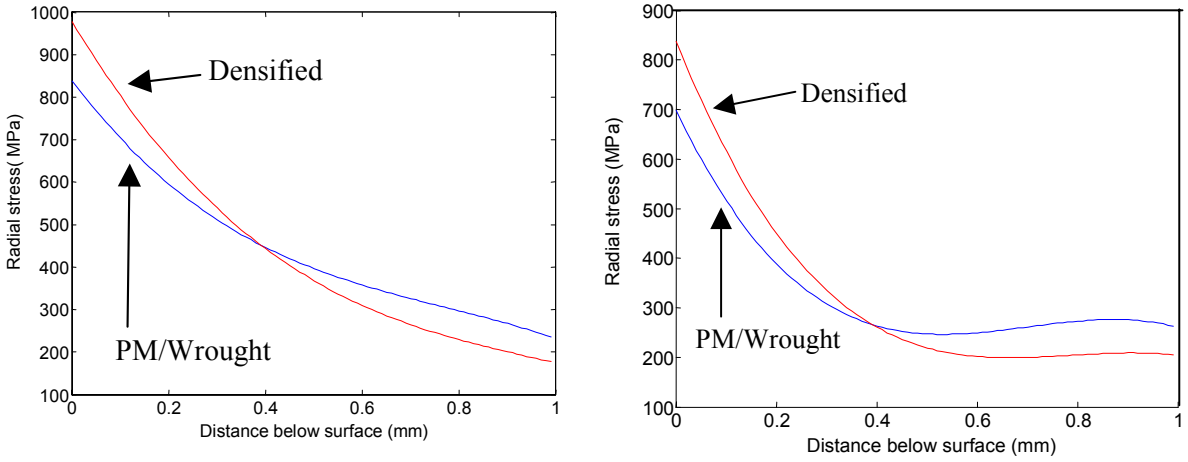


a) *b)*

Figure 3. a) Residual stress from FEA and curve fitted stress field. b) Path where the data in figure 3a is sampled.

Using the technique previously described to obtain residual stress the stress field becomes a step function, see figure 3a. To avoid this, a curve fit is performed from the FE results to model a smoother more realistic stress field that conforms to measurements. Figure 3b depicts a critical section where the radial tensile stresses from bending are the highest and where a tooth root fatigue failure is likely to occur. This is also where the stress data in figure 3a is sampled.

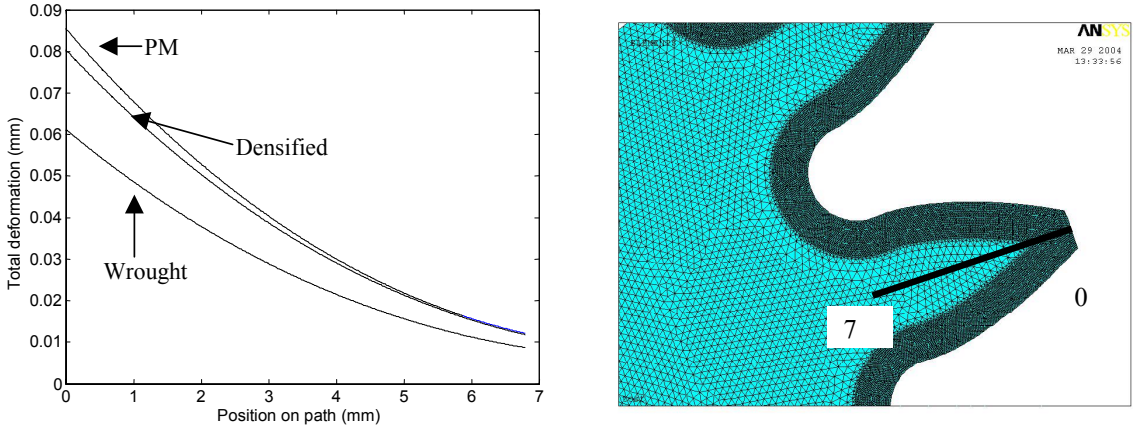
If the gear tooth is subjected to a point load according to figure 2b the radial stress along the path in figure 3b is depicted in figure 4a. Figure 4b shows the radial stress after the residual stress has been superimposed on the radial stress thus demonstrating the beneficial effects from case hardening. The result for a uniform density PM gear tooth is identical to a gear tooth in wrought material, which is in accordance with beam theory. However, for a densified PM gear tooth the result is different since E and ν vary.



a) *b)*

Figure 4. a) Radial stresses on critical path for surface densified PM gear tooth and PM/wrought material gear tooth. b) Same as in a) but residual stresses added.

From figure 4 it is evident that the surface densified material has better static and dynamic properties than its wrought counterpart for equal mechanical performance due to the alloying content.

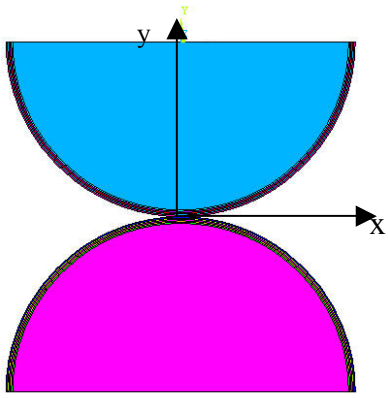


a) *b)*

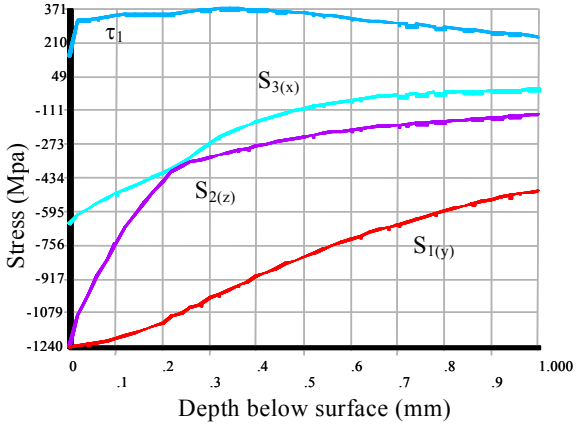
Figure 5. a) Deformation from bending of tooth along path. b) Path sketched on FE mesh.

Figure 5a shows the total deformation along the path depicted in figure 5b. The densification has little influence on the bending deformation of the tooth. This means that attention has to be paid to the deflection when using PM steel in order to avoid interference. A more flexible tooth is often desired to decrease noise levels in transmissions. Special software is needed to calculate the profile since it will deviate from the involute. For wrought steel there is often a compromise between strength and slenderness. With densified PM a silent yet strong tooth is obtainable.

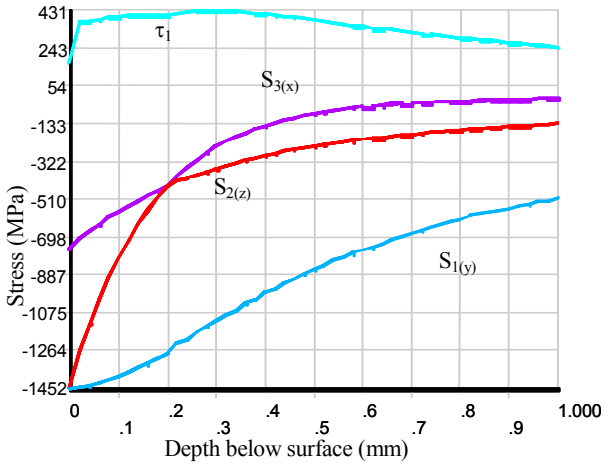
The contact model simulates the conditions at the pitch point of two identical teeth, there is no sliding and no tangential stresses on the surface at the pitch point. The surfaces are smooth and there is no lubricant film separating the surfaces since there is no relative sliding. The model with layers is depicted in figure 6a. Plain strain is assumed and no residual stresses unless indicated otherwise.



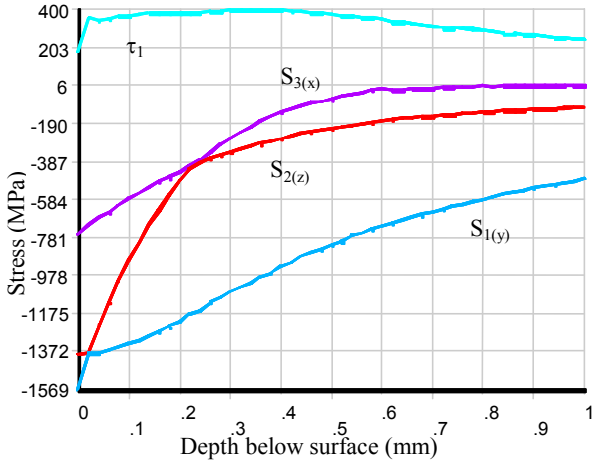
a)



b)

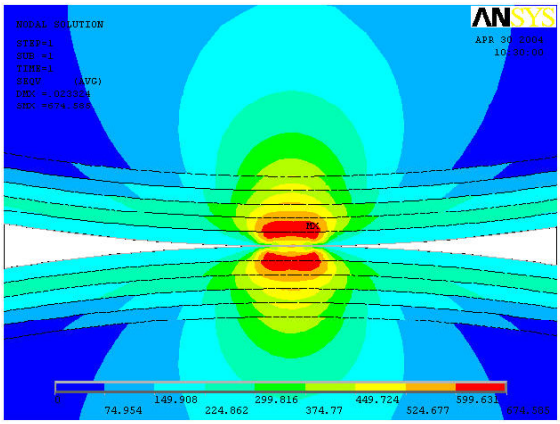


c)

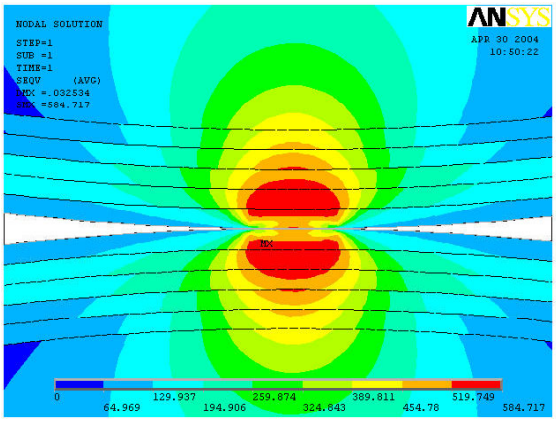


d)

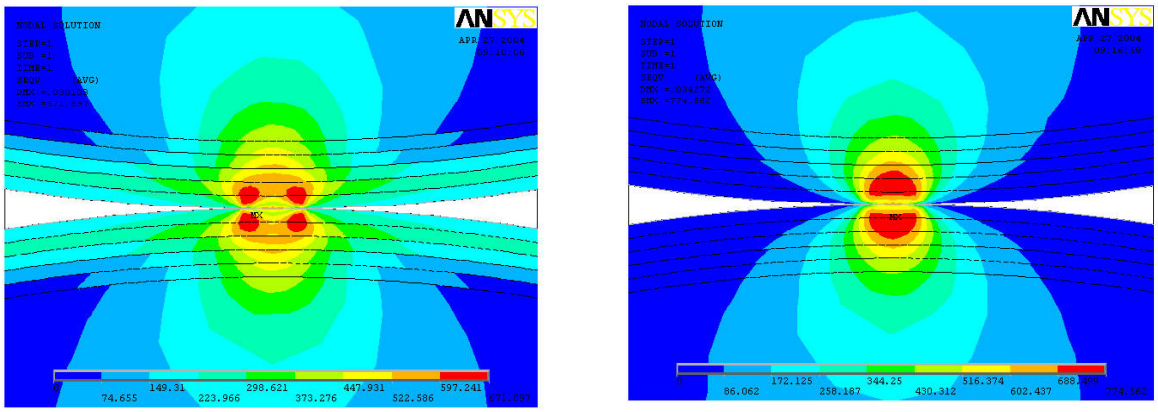
Figure 6. a) Geometry in calculations. b) Principal stresses in centre of contact (y=0), PM steel. c) Principal stresses wrought material. d) Principal stresses densified PM-steel. τ_1=Principal shear stress, $\sigma_{1,2,3}$=Principal stress 1,2,3 coinciding with y,z,x-axis



a)



b)



c) *d)*

Figure 7. von Mise's stress. a) Wrought steel with residual stress according to figure 3a. b) PM steel with residual stress. c) Densified PM with res. stress. d) Densified PM no res. stress.

In figure 6, the PM material has its maximum shear stress further down into the material. Densified PM shows higher compressive stresses in the x-direction than in the y-direction, even higher than wrought steel. This is due to the drop in shear modulus. Figure 7 depicts the von Mise's stresses under the contact. The residual stress pushes the maximum away from the centre of the contact and upwards and 2 local maximums occur. This effect is more pronounced in densified PM due to the increased strain since sub-layers deform more than the top layer. The maximum von Mise's stress will be equally high for a densified PM steel as for wrought steel. PM steel displays lower von Mise's stress in a larger volume. The results were found to be sensitive to ν and small variations will affect contact stresses greatly.

Conclusions

FE calculations show that surface densification creates a higher maximum root stress compared to non densified PM/wrought steel due to the gradient in E and υ. This means that a higher core density will have a positive impact on the stress state of a densified gear tooth. The deflection of the teeth is little affected by densification. Subsurface stresses in a densified and case hardened material will have a different distribution compared to PM/wrought steel due to the increased strain in sub-layers.

References:

[1] McAdam. (1951) Some relations to powder characteristics to the elastic modulus and shrinkage of sintered ferrous compacts, *J. Iron Steel Inst.,* Vol. 168, pp346-348.

[2] H. Kolaska.(2003) Pulvermetallurgie in Wissenschaft und Praxis, Band 19, pp 7, ISBN 3-933842-67-0

[3] S. Pehan, T. K. Hellen, J. Flasker, S. Glodez. (1997) Numerical methods for determining stress intensity factors vs. crack depth in gear teeth roots, *Int. J Fatigue,* Vol. 19, No. 10, pp 667-685.

[4] L. Fredette & M. Brown. (1997) Gear Stress Reduction Using Internal Stress Relief Features, *J. of Mech. Design,* Vol. 119.

[5] H. v. Eiff, K.H Hirschman & G. Lechner. (1990) Influence of Gear Tooth Geometry on Tooth Stress of External and Internal Gears, *J. of Mech. Design,* Vol. 112.

[6] E. McEwen. (1949) Stresses in elastic cylinders in contact along a generatrix, *Philosophical Magazine,* Vol.40, pp 454.

[7] Hugnell, A.B.J., Björklund, S. and Andersson, S. (1996) Simulation of the Mild Wear in a Cam-Follower Contact with Follower Rotation. *Wear* 199, pp 202-210.